Molecular Therapy
Oncolytics
Original Article

DAP10 integration in CAR-T cells enhances the killing of heterogeneous tumors by harnessing endogenous NKG2D

Shanglin Li,[1,2,13] Ruocong Zhao,[3,12,13] Diwei Zheng,[1,2] Le Qin,[1] Yuanbin Cui,[1,2] Yao Li,[1,2] Zhiwu Jiang,[1] Mengjun Zhong,[3] Jingxuan Shi,[1] Ming Li,[4] Xindong Wang,[5] Zhaoyang Tang,[6,7] Qiting Wu,[1] Youguo Long,[1] Duo Hu,[5] Suna Wang,[1] Yao Yao,[1] Shuang Liu,[8] Li-Hua Yang,[9] Zhenfeng Zhang,[10] Qiannan Tang,[11] Pentao Liu,[11] Yangqiu Li,[3] and Peng Li[1,5,12]

[1]China-New Zealand Joint Laboratory of Biomedicine and Health, State Key Laboratory of Respiratory Disease, Guangdong Provincial Key Laboratory of Stem Cell and Regenerative Medicine, Key Laboratory of Stem Cell and Regenerative Medicine, Guangzhou Institutes of Biomedicine and Health, Chinese Academy of Sciences, Guangzhou, China; [2]University of Chinese Academy of Sciences, Beijing, China; [3]Institute of Hematology, Medical College, Jinan University, Guangzhou, China; [4]Anhui University, Hefei, China; [5]Bioland Laboratory, Guangzhou Regenerative Medicine and Health Guangdong Laboratory, Guangzhou, China; [6]Guangdong Zhaotai InVivo Biomedicine Co., Ltd., Guangzhou, China; [7]Guangdong Zhaotai Cell Biology Technology, Ltd., Foshan, China; [8]Department of Hematology, Guangdong Second Provincial General Hospital, Guangzhou, China; [9]Department of Pediatric Hematology, Zhujiang Hospital, Southern Medical University, Guangzhou, Guangdong, China; [10]Department of Radiology, Translational Provincial Education Department Key Laboratory of Nano-Immmunoregulation Tumor Microenvironment, The Second Affiliated Hospital of Guangzhou Medical University, Guangzhou, China; [11]School of Biomedical Sciences, Stem Cell and Regenerative Medicine Consortium, Li Ka Shing Faculty of Medicine, The University of Hong Kong, Hong Kong SAR, China; [12]Centre for Regenerative Medicine and Health, Hong Kong Institute of Science & Innovation, Chinese Academy of Sciences, Hong Kong SAR, China

Although chimeric antigen receptor T (CAR-T) cells have achieved remarkable successes in hematological malignancies, the efficacies of CAR-T cells against solid tumors remains unsatisfactory. Heterogeneous antigen expression is one of the obstacles on its effective elimination of solid cancer cells. DNAX-activating protein 10 (DAP10) interacts with natural killer group 2D (NKG2D), acting as an adaptor that targets various malignant cells for surveillance. Here, we designed a DAP10 chimeric receptor that utilized native NKG2D on T cells to target NKG2D ligand-expressing cancer cells. We then tandemly incorporated it with anti-glypican 3 (GPC3) single-chain variable fragment (scFv) to construct a dual-antigen-targeting system. T cells expressing DAP10 chimeric receptor (DAP10-T cells) displayed with an enhancement on both cytotoxicity and cytokine secretion against solid cancer cell lines, and its tandem connection with anti-GPC3 scFv (CAR GPC3-DAP10-T cells) exhibited a dual-antigen-targeting capacity on eliminating heterogeneous cancer cells *in vitro* and suppressing the growth of heterogeneous cancer *in vivo*. Thus, this novel dual-targeting system enabled a high efficacy on killing cancer cells and extended the recognition profile of CAR-T cells toward tumors, which providing a potential strategy on treatment of solid cancer clinically.

INTRODUCTION

Chimeric antigen receptor T (CAR-T) therapy has been applied on treating certain types of hematological malignancies successfully,[1–3] but the efficacy of it on curing patients with solid tumors remains problematic. The poor recognition of heterogeneous antigens expressed on solid tumors is one of the critical impediments on efficient CAR-T therapy.[4–6]

The activating receptors expressed on natural killer cells recognize diverse ligands expressed on variety of malignant cells.[7–10] Of them, natural killer group 2 D (NKG2D) is a type II membrane-oriented transmembrane receptor that is expressed on both NK cells and a majority proportion of CD8+ T cells. The membrane localization and signal transduction of NKG2D depend on another protein, DNAX-activating protein 10 (DAP10).[11,12] Despite that NK-cell-expressing NKG2D has been well recognized for its function of meditating the immunosurveillance of malignant cells,[13,14] NKG2D on T cells conducts its function in a milder manner and may only serves as a costimulatory signal.[15,16] Functional enhancement of NKG2D on T cells is a potential approach to confer the CAR-T cell with

Received 29 April 2022; accepted 1 June 2022;
https://doi.org/10.1016/j.omto.2022.06.003.

[13]These authors contributed equally

Correspondence: Yangqiu Li, PhD, Institute of Hematology, Medical College, Jinan University, Guangzhou, China.
E-mail: yangqiuli@hotmail.com
Correspondence: Peng Li, PhD, China-New Zealand Joint Laboratory of Biomedine and Health, State Key Laboratory of Respiratory Disease, Guangdong Provincial Key Laboratory of Stem Cell and Regenerative Medicine, Key Laboratory of Stem Cell and Regenerative Medicine, Guangzhou Institutes of Biomedicine and Health, Chinese Academy of Sciences, Guangzhou, China.
E-mail: li_peng@gibh.ac.cn

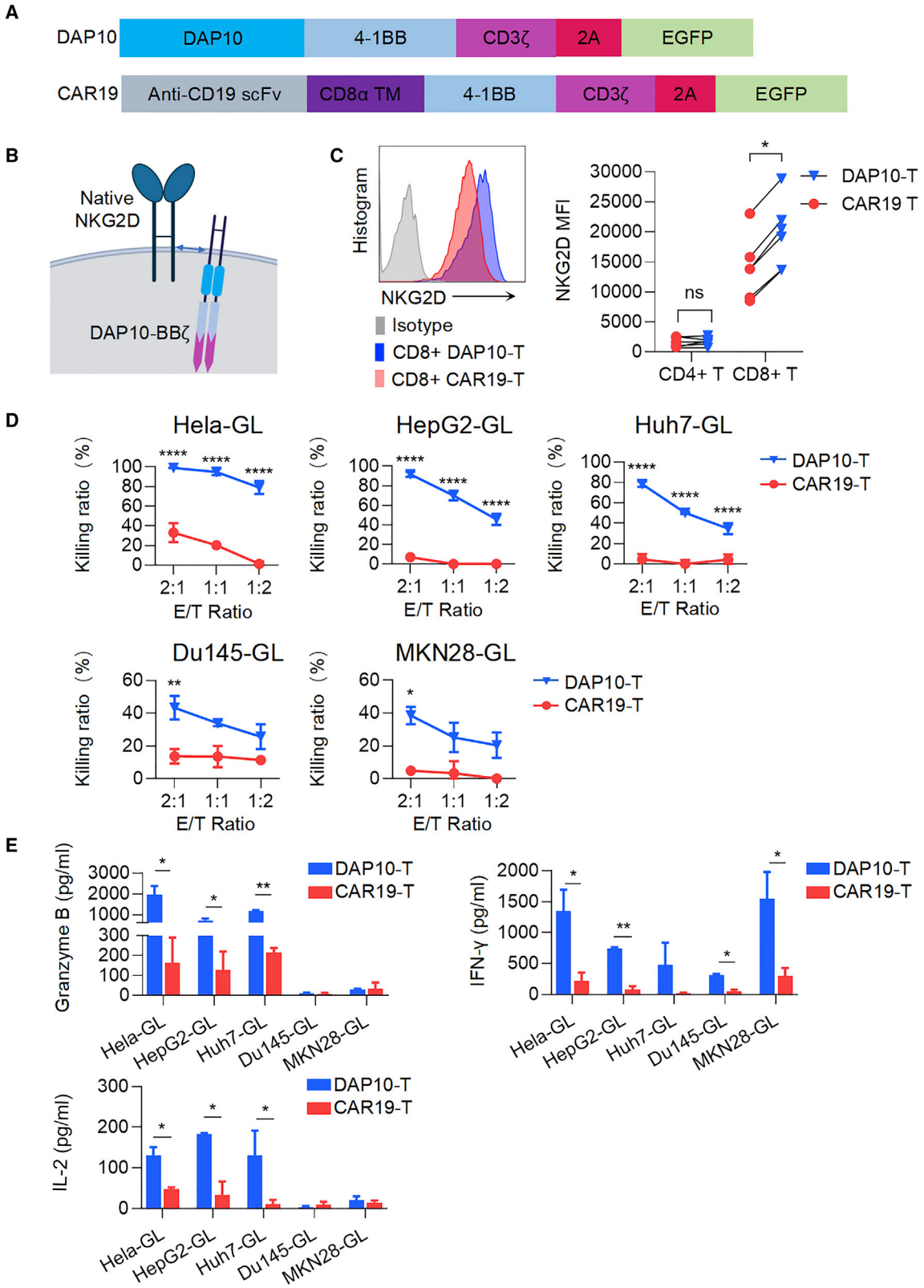

(legend on next page)

NK-like killing activity that increases their efficiency on eliminating tumor cells, especially the ones with the antigen loss.

In this study, we demonstrated that NKG2D expressed on T cells was functionally less efficient compared with that expressed on peripheral NK cells. We then designed a recombinant molecule as DAP10-4-1BB-CD3z, and expression of it enabled T cells (DAP10-T) to trigger a robust immune response against various solid cancer cells via binding to NKG2D. We subsequently incorporated this DAP10 fragment tandemly with a second-generation CAR targeting GPC3, termed CAR GPC3-DAP10, which exhibited a dual specificity against cancer cells both *in vitro* and *in vivo*. More importantly, we found that the incorporation of DAP10 with the GPC3-CAR eliminated cancer cells that expressed heterogeneous antigens more efficiently. To date, our study is the first to report the incorporation of an NKG2D-harnessing fragment with a single-chain variable fragment (scFv)-derived CAR fragment to confer the NK-like killing capacity to CAR-T cells. Therefore, we provide a novel CAR-T cell-based therapeutic approach that boosts anti-tumor immune responses, by resolving the issue of antigen escape, for the application of it on treating solid cancers.

RESULTS

Killing activity of DAP10-T cells against various cancer cells is dependent on the NKG2D expression

To study the role of NKG2D expressed on CAR-T cells, we firstly examined the distribution of NKG2D expressions on T cells. A large proportion of freshly isolated CD8+ T cells expressed NKG2D, and its expression level was significantly increased upon CD3/CD28 antibody stimulation. In contrast, CD4+ T cells expressed a low level of NKG2D (Figures S1A and S1B).

To determine whether the killing activity contributed by native NKG2D, CD8+ T cells or NK cells were incubated with NKG2D-sensitive cancer cell lines including Huh7-GPF-2A-luciferase (GL) and Hela-GL. The killing activity of CD8+ T cells was much lower compared with that of NK cells (Figures S1C and S1D). Blocking of NKG2D with anti-NKG2D antibody diminished the killing capacity of NK cells significantly, while it had an almost negligible effect on that of CD8+ T cells (Figures S1C and S1D). Accordingly, granzyme B (Figure S1E) and interferon gamma (IFN-γ) (Figure S1F) secreted by NK cells were significantly reduced when NKG2D was blocked, while no significant influence was observed in the CD8+ T cells. These results suggested that the activation of NKG2D can trigger effector functions in NK cells, but that its function is not strong in T cells.

To enhance the NKG2D-mediated signaling on CD8+ T cells for improving its tumor-killing activity, we transduced T cells with a recombinant molecule. This recombinant molecular (DAP10BBz) expressed the full length of DAP10 that fused with the endoplasmic 4-1BB and CD3ζ activation domains (Figures 1A and 1B). Flow cytometry was applied to evaluate the surface expression of NKG2D; CD8+ T cells transduced with this DAP10BBz molecule (DAP10-T) significantly elevated NKG2D expression level on CD8+ T cell surface (Figure 1C), suggesting a role of DAP10 on supporting the membrane localization of NKG2D. We checked the expression levels of NKG2D ligands, including MICA, MICB, and ULBP1-3, on multiple solid cancer cell lines (Figure S2) and utilized them as targeted cancer cells to examine the effector functions of DAP10-T cells by cytotoxicity assays. DAP10-T cells lysed multiple cancer cells with a significant higher efficiency than anti-CD19 CAR-T cells (CAR19-T) (Figure 1D). Accordingly, the secretion of cytokines, including granzyme B, IFN-γ, and interleukin-2 (IL-2) (Figure 1E), was also significantly increased in DAP10-T cells compared with CAR19 T cells. Altogether, these results suggested that the transduction of T cells with our modified DAP10 vector enhanced their tumor-killing activity through NKG2D-mediated recognition of its ligands in tumor cells.

To investigate whether these anti-tumor effects were dependent on endogenous expression of NKG2D on T cells, CD8+ or CD4+ T cells were isolated for a killing assay against HeLa-GL target cells. The results showed that CD8+ T cells exhibited a high efficiency on tumor cell killing and that the killing activity of CD8+ DAP10-T cells was significantly higher than that of CD8+ CAR19-T cells (Figure S3A). CD4+ T cells, however, showed an overall much lower efficiency, and the killing activity of DAP10-T cells were comparable with that of CAR19-T in CD4+ T cell subset (Figure S3B). We then utilized an anti-NKG2D antibody to block NKG2D in T cells, and the blockade of NKG2D dramatically compromised the tumor-killing activity of DAP10-T cells (Figure S3C). In sum, these results demonstrated that overexpression of the recombinant DAP10BBz molecule increased the killing efficiency of CD8+ T cells toward a variety of solid cancer cells in an NKG2D-dependent manner.

Tandem incorporation of the DAP10 fragment in a GPC3-CAR confers the T cells with the capacity to kill both GPC3+ and GPC3- cancer cells

The transduction of DAP10BBz enhanced the tumor-killing activity of T cells; next, we sought to incorporate this fragment expressing DAP10BBz into a traditional CAR for acquiring a dual-antigen-targeting function for recognizing heterogeneous cancer cells. We tandemly linked DAP10BBz with an scFv targeting GPC3, which expressed in

Figure 1. Killing activity of DAP10-T cells against various cancer cells

(A) Schematic diagram of the structures of CAR gene-expression cassettes. (B) Schematic diagram for the expression of DAP10BBz with native NKG2D on T cell membrane. Arrows represent the interaction of NKG2D and DAP10. (C) Expression of NKG2D on CD4+ and CD8+ T cells after DAP10BBz gene transduction detected by flow cytometry. The histogram plot (left) shows one representative experiment from 6 different donors, and the data of NKG2D mean fluorescence intensity (MFI) in CAR-T cells from 6 donors were plotted (right). (D) Results of killing assays performed with DAP10-T cells against multiple solid cancer cell lines. The results shown are from one representative experiment out of two independent experiments with 2 different donors. (E) Detection of granzyme B, IFN-γ and IL-2 secretion by DAP10-T cells and CAR19-T cells stimulated by multiple solid cancer cell lines. Error bars denote the SEM, and the results were compared with Student's t test. *$p < 0.05$, **$p < 0.01$, ***$p < 0.001$, ****$p < 0.0001$.

75% of hepatocellular carcinomas (HCCs),[17] termed GPC3-DAP10 CAR (Figures 2A and 2B). We transduced plasmids either expressing GPC3-DAP10 CAR or GPC3-targeted CAR into T cells and found no significant differences in the transduction efficiency between the two CAR-T groups (Figure S4A). We subsequently investigated whether the effector functions of DAP10BBz were affected by this tandem incorporation by performing cytotoxicity and cytokine secretion assays with transduced T cells and HeLa-GL cells, which highly expressed NKG2D ligands but lacked GPC3 expression. The results showed that the cytotoxicity of DAP10-T and CAR GPC3-DAP10-T cells against HeLa cancer cells was at a comparably high level (Figure S4B). They also produced much higher level of cytokines than those in CAR19-T and CAR GPC3-T cells. CAR GPC3-DAP10 T cells produced comparable levels of IFN-γ, while the levels of granzyme B and IL-2 were slightly reduced compared with the DAP10-T cells group (Figure S4C). These results demonstrate that tandem incorporation of DAP10 in GPC3-CAR can basically maintain their capacity to recognize NKG2D ligand+tumor targets.

Next, we evaluated the effector functions of CAR GPC3-DAP10-T cells against liver cancer cells that express GPC3. CAR GPC3-DAP10-T cells killed GPC3+ Huh7-GL hepatocellular cancer cells with comparable efficiency with CAR GPC3-T cells (Figure 2C). Strikingly, CAR GPC3-DAP10-T cells also exhibited a high cytotoxicity against SK-Hep1-GL cells, which are GPC3-, while the traditional GPC3-T cells had no killing activity (Figure 2C). The effective tumor-killing activity of CAR GPC3-DAP10-T cells was accompanied by the production of cytokines including granzyme B (Figure 2D), IFN-γ (Figure 2E), and IL-2 (Figure 2F).

Since CD4+ T cells generally express quite low levels of NKG2D, CD4+ DAP10-T cells are unable to be redirected by DAP10 CAR (Figure S3B). However, CD4+ CAR GPC3-DAP10-T cells harbor GPC3-scFv and could be redirected and activated by GPC3 tumor antigen, as CD4+ CAR GPC3-DAP10-T cells dramatically upregulated both CD25 and CD69, which are recognized as classical T cell-activation biomarkers, after being cocultured with Huh7 GPC3+ hepatocellular cancer cells compared with CD4+ CAR19-T cells (Figures S4D and S4E). CD4+ CAR GPC3-T cells and CD4+ CAR GPC3-DAP10-T cells also exhibited significantly higher levels of cytotoxicity than CD4+ CAR19-T cells (Figure S4F). These results suggested that GPC3-DAP10 CAR functions through anti-GPC3 scFv in CD4+ T cells. Taken together, these results demonstrated that CAR GPC3-DAP10 T cells possess the capacity to target GPC3+ and NKG2D-sensitive liver cancer cells *in vitro*.

Efficient elimination of GPC3 heterogeneous cancer cells by CAR GPC3-DAP10 T cells

To further characterize the anti-heterogeneous tumor function of CAR GPC3-DAP10-T cells, we utilized a system comprised of tumor cells expressing heterogeneous antigens. In this system, a proportion of SK-Hep1 cancer cells were transduced with lentivirus-expressing GPC3 and tdTomato as GPC3+tdTomato+ cells, while another part of SK-Hep1 cells were GPC3 negative but expressed EGFP (GPC3-EGFP+). We then cocultured these mixed SK-Hep1 tumor cells (Figure 3A) with CAR19-T, DAP10-T, CAR GPC3-T, or CAR GPC3-DAP10-T cells to assess their tumor-killing activity. We detected the remaining live cancer cells with fluorescence microscopy and quantified fluorescent cells in several views selected from diagonal lines of montage photos (Figure 3B). Fluorescent microscopy images and image quantification showed that the amount of both GPC3+tdTomato+ and GPC3-EGFP+ cancer cells was significantly reduced by DAP10-T cells compared with CAR-19 T cells (Figures 3B and 3C). CAR GPC3-T cells elicited a more efficient killing toward GPC3+ cells (tdTomato+) than GPC3- cells (EGFP+), indicating that GPC3- tumor cells escaped from its restriction (Figures 3B and 3C). Interestingly, unlike DAP10-T or CAR GPC3-T, CAR GPC3-DAP10-T cells showed a high and similar efficiency on eliminating both GPC3+ (tdTomato+) and GPC3- (EGFP+) cancer cells (Figures 3B and 3C). Taken together, while GPC3- SK-Hep1 cells escaped from the killing of CAR GPC3-T cells, they were efficiently targeted and killed by CAR GPC3-DAP10-T cells, which demonstrates that the combination of DAP10BBz with anti-GPC3 scFv extended its capability to eliminate the cancer cells with heterogeneous antigens.

CAR GPC3-DAP10-T cells exhibit a dual-antigen-targeting capacity and eliminate heterogeneous tumors *in vivo*

To test the anti-tumor activity of CAR GPC3-DAP10-T cells *in vivo*, we utilized a xenograft mouse model in which HeLa cells were subcutaneously inoculated into immunodeficient NOD-SCID IL-2Rγ$^{-/-}$ (NSI) mice.[18] The HeLa cells induced the formation of NKG2D-sensitive tumors. Fourteen days later, DAP10-T, CAR19-T, CAR GPC3-T, and CAR GPC3-DAP10-T cells were injected into these mice intravenously to examine their anti-tumor activities (Figure 4A). The results showed that DAP10-T and CAR GPC3-DAP10-T cells restricted the growth of the HeLa tumor more efficiently than CAR19-T or CAR GPC3-T cells (Figures 4B and 4C), indicated by the slow growth of both tumor nodule volume (Figure 4C) and tumor weight (Figure 4D).

To further determine whether the tandem connection with DAP10 interferes with the anti-tumor activity of the GPC3 CAR *in vivo*, we subsequently constructed a highly aggressive GPC3-expressing Huh7 cell HCC mouse model (Figure 4E). Similarly, CAR GPC3-DAP10-T cells conducted a highly efficient tumor-killing activity toward tumors formed with GPC+ Huh7 cells, and the efficiency was comparable with that of GPC3-T but significantly higher than CAR19 or DAP10-T cells (Figures 4F and 4G), and the tumor weights were lower in CAR GPC3-DAP10-T cell and CAR GPC3-T cell groups compared with the CAR19-T cell group (Figure 4H), suggesting that the incorporation of the DAP10 fragment in GPC3 did not interfere with the recognition capacity of the GPC3 CAR.

To model the cancer-expressing heterogeneous antigens *in vivo*, we established a xenograft in which tumors were formed by a mixture of GPC3+ and GPC3- SK-Hep1 cells. We then used this mouse to evaluate the tumor-killing activity of CAR GPC3-DAP10-T cells (Figure 5A). Strikingly, only CAR GPC3-DAP10-T cells conducted an efficient

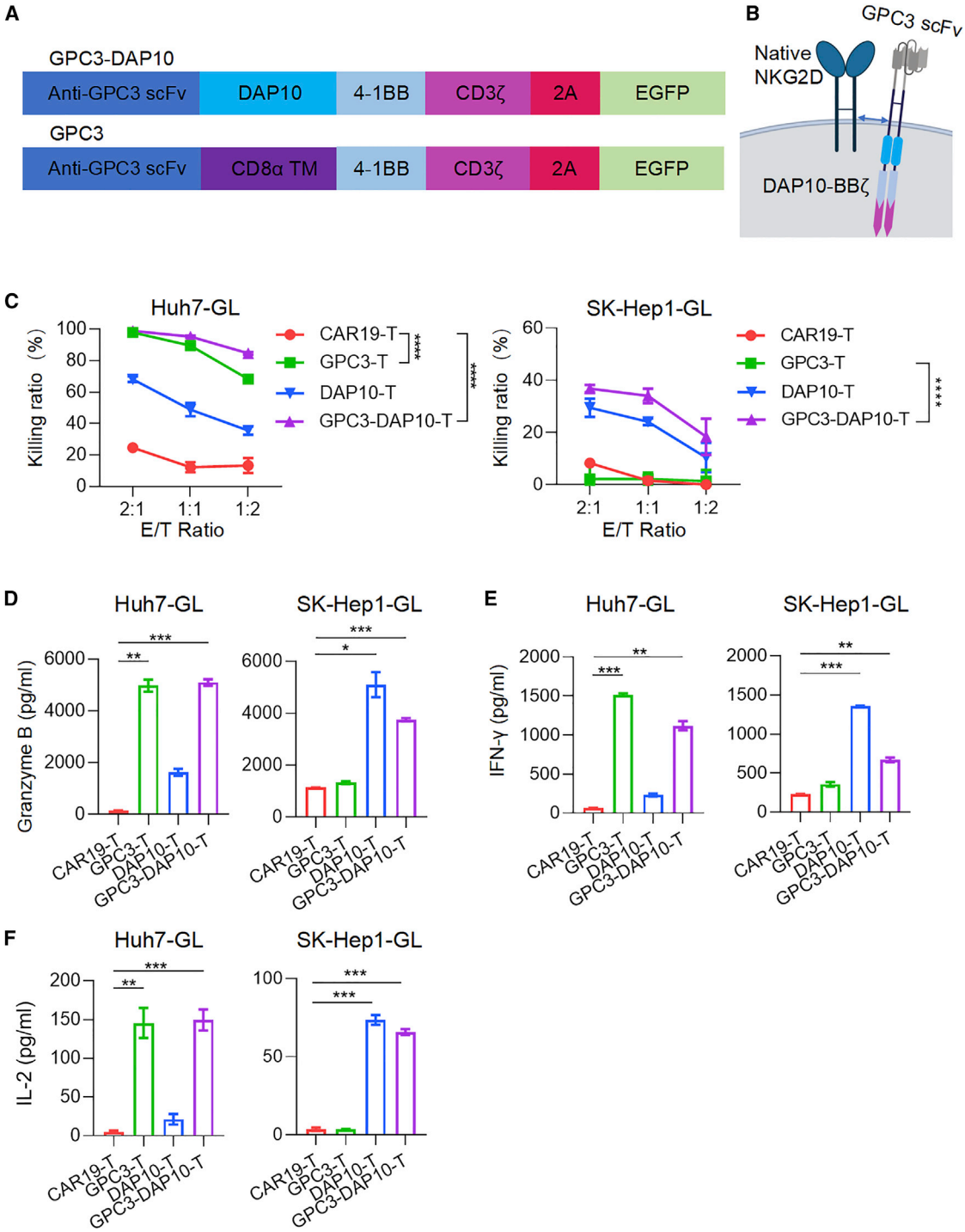

Figure 2. Tandem incorporation of DAP10BBz fragment with GPC3-scFv confers T cell killing capacity against both GPC3+ and GPC3- cancer cells

(A) Schematic diagram of the structures of GPC3 CAR and GPC3-DAP10 CAR gene-expression cassettes. (B) Schematic diagram for the expression of GPC3-DAP10BBz with native NKG2D on T cell membrane. Arrows represent the interaction of NKG2D and DAP10. (C) Results of killing assays of CAR19-T, CAR GPC3-T, DAP10-T, and CAR GPC3-DAP10-T cells against Huh7-GL and SK-Hep1-GL cancer cell lines. The results shown are from one representative experiment out of two independent experiments with 2 different donors. (D) Detection of granzyme B secretion by T cells stimulated by Huh7-GL and SK-Hep1-GL cancer cell lines. (E) Detection of IFN-γ secretion by T cells stimulated by Huh7-GL and SK-Hep1-GL cancer cell lines. (F) Detection of IL-2 secretion by T cells stimulated by Huh7-GL and SK-Hep1-GL cancer cell lines. The killing results were compared with two-way ANOVA with Tukey's multiple comparisons test. Student's t test was used to compare cytokines secretion. Error bars denote the SEM. *$p < 0.05$, **$p < 0.01$, ***$p < 0.001$, ****$p < 0.0001$.

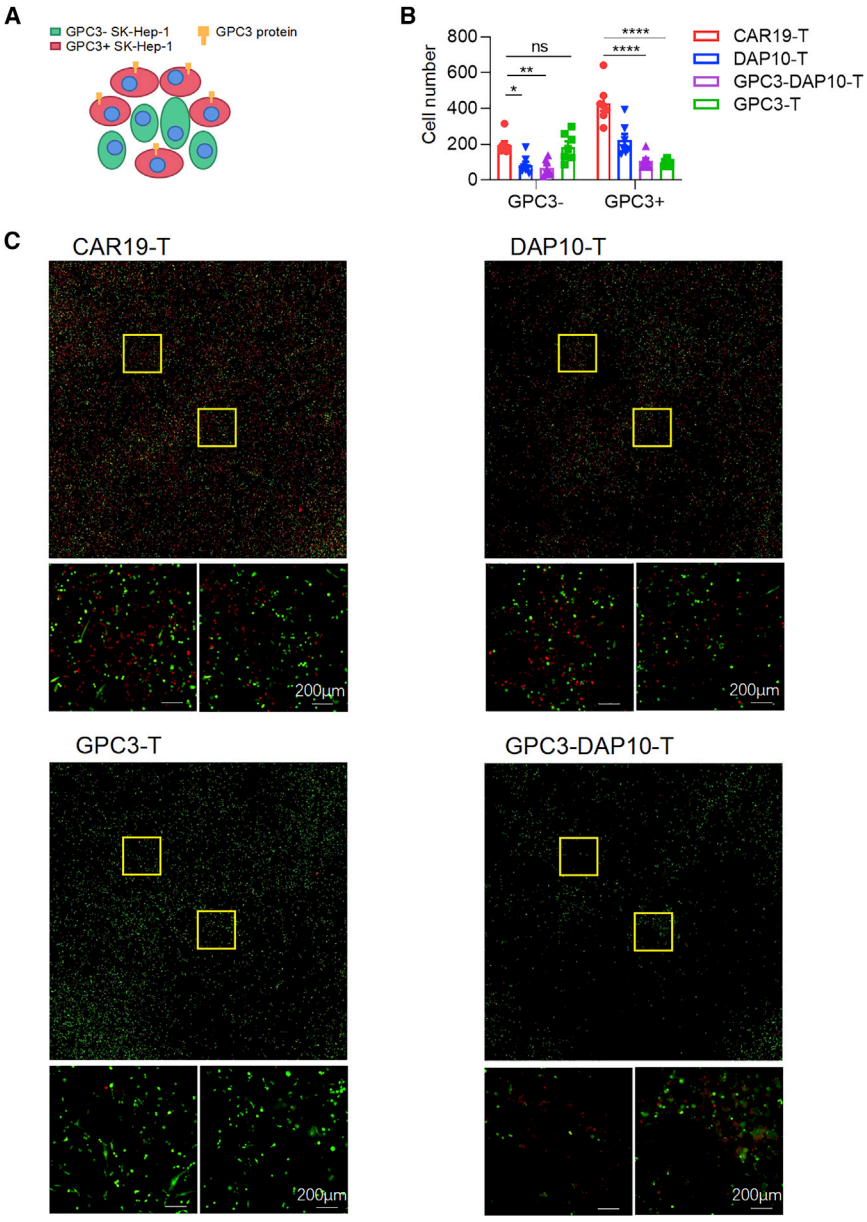

Figure 3. Efficient elimination of GPC3 heterogeneous cancer cells by CAR GPC3-DAP10-T cells

(A) Schematic diagram of SK-Hep1 heterogeneous cancer cells. The GPC3+ (labeled by tdTomato) and GPC3- (labeled by EGFP) SK-Hep1 were mixed (ratio, 2:1) to mimic the heterogeneous cancer cells. The CAR-T cells (1×10^5) cocultured with heterogeneous SK-Hep1 (1×10^5) for 24 h in a 24-well plate, followed by imaging. (B) GPC3+ (red) and GPC3- (green) cancer cell counts after coculture with CAR19-T, DAP10-T, CAR GPC3-T, and CAR GPC3-DAP10-T cells. Seven individual photos on diagonal lines were used to calculate cell counts for one montage photo. (C) The overall plate images of indicated CAR-T cells. 8 × 8 photos for each CAR-T cells made one montage. The two yellow squares on montage photos indicate tow zoom-in photos below the montages. Scale bar, 200 μm. Error bars denote the SEM, and the results were compared with Student's t test. *p < 0.05, **p < 0.01, ***p < 0.001, ****p < 0.0001.

tumor restriction on the tumor, as the growth of the tumor volume (Figures 5B and 5C) and weight (Figure 5D) were dramatically inhibited. All other CAR-T cells including CAR19-T, DAP10-T, or CAR GPC3-T cells showed negligible effects on tumor growth (Figure 5B). Furthermore, a higher number of CAR-T accumulation was observed in the CAR GPC3-DAP10-T cell-treated mice, prompting improved T cell persistence caused by the dual-targeting strategy (Figure 5E). Collectively, these results suggested that the strategy with a tandem combination of anti-GPC3 scFv with DAP10BBz exhibited a dual-antigen-targeting capacity that enhanced the efficiency on restricting the tumor growth, especially the tumor with heterogeneous antigen expression, by targeting both GPC3+ and GPC3- cancer cells.

Taken together, these results revealed that CAR GPC3-DAP10 T cells can impair the growth of NKG2D-sensitive and GPC3+ cells *in vivo*. Importantly, CAR GPC3-DAP10 T cells showed potential capacity to eliminate heterogeneous tumor *in vivo*.

DISCUSSION

The heterogeneous antigen expression of solid cancers prevents CAR-T cells from eliminating all cancer cells and hinders CAR-T cells from producing sufficiently strong immune responses.[19–21] To solve this problem, previous studies have developed dual- or triple-connected scFv-targeting CARs, which enable the CARs to recognize two or even three tumor-associated antigens.[22] Here, we designed a recombinant DAP10 CAR that was able to redirect T cells to recognize NKG2D ligands expressed by various cancer cells. We then incorporated this receptor in tandem with a traditional CAR targeting GPC3, the GPC3-DAP10 CAR, which exhibited a dual function which are the recognition function mediated by GPC3 and activating NKG2D signaling via DAP10. More importantly, this GPC3-DAP10 CAR enabled T cells to effectively eliminate heterogeneous cancer cells and thus provided a novel approach to kill heterogeneous cancer cells that normally escape from the restriction by CAR-T therapy.

Previous studies have reported the utilization of NKG2D-based CAR-T/NK cells against multiple cancers,[23–25] and some studies have achieved substantial clinical responses.[26,27] However, there are no reports for the combination of NKG2D CAR with scFv-based CARs yet.

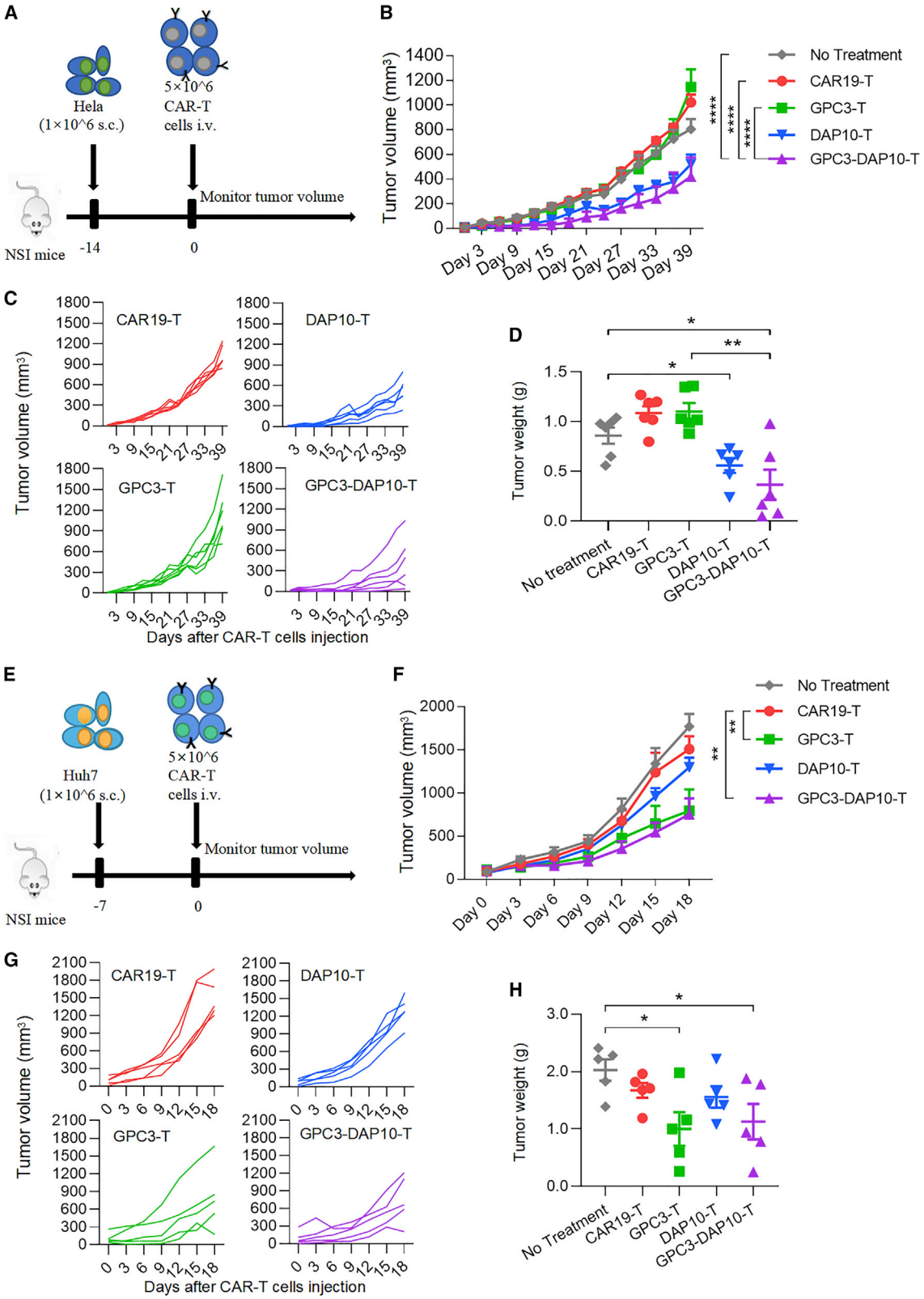

(legend on next page)

One important reason is that NKG2D is a type II lectin receptor with a C terminus extracellularly and an N terminus intracellularly located;[11] this opposite orientation makes it difficult to be tandemly linked with scFv. In this study, we managed to incorporate DAP10, instead of NKG2D, with scFv, as DAP10 was a much smaller type I membrane molecule, which activated NKG2D.

The ligands recognized by NKG2D included stress-inducible ligand family members such as MICA, MICB, and ULBPs. These ligands have been reported to be induced by various strategies. Certain types of chemotherapeutic drugs and epigenetic inhibitors are applied to induce NKG2D ligands. Previous studies showed that sodium valproate could induce the expression of NKG2D ligands, including MICA, MICB and ULBP1-3,[28–30] and proteasome inhibitors can induce the expression of ULBP2 in hematological malignancy cells.[31] Abruzzese et al. reported that inhibition of bromodomain and extra-terminal (BET) proteins upregulated the expression of the NKG2D ligand MICA in multiple myeloma cells, which increased their sensitivity to NK cell-mediated cytotoxicity.[32] Taken together, these studies suggested that the chemical drugs can induce the expression of NKG2D ligands in cancer cells for the NKG2D/DAP10 receptor to target. The strategy we designed here, which tandemly incorporated the DAP10 fragment into CAR, may enhance the compatibility of CAR-T cells with chemical drugs and further improve the anti-tumor efficacy against solid cancers.

Although CD4+ T cells cannot utilize DAP10BBz to invoke NKG2D-dependent cytotoxic function, GPC3-DAP10 CAR can endow the capacity to killing GPC3+tumor cells to CD4+ T cells. We suppose there is a structural hindrance that may impact the activation-signaling intensity between endogenous NKG2D and GPC3-DAP10 CAR, as we observed lower levels of cytokine secretion in CAR GPC3-DAP10 T cells compared with DAP10-T cells (Figures 2D and 2E). The detailed mechanism underlying this phenomenon awaits further study.

Moreover, our designed CAR combined with DAP10 and GPC3-CAR provides a promising method to overcome the obstacle on killing tumors with antigen heterogeneity. The results from tumor mouse models in this study lay a foundation for developing this novel CAR-T cell as therapeutic approaches in clinical settings.

MATERIAL AND METHODS

Cell lines and cell culture conditions

HEK-293T cells were maintained in Dulbecco's modified Eagle's medium (DMEM) (Gibco, Grand Island, NY, USA). MKN28 gastric cancer cells were cultured in RPMI-1640 medium (Gibco). DMEM and RPMI-1640 medium were supplemented with 10% FBS, 2 mM L-glutamine, 100 U/mL penicillin, and 100 mg/mL streptomycin. The cell lines Huh7, HepG2, SK-Hep1, HeLa, and DU145 were cultured in DMEM (Gibco). All the target cell lines were transduced with GFP-2A-luciferase to measure cell viability during coculture with CAR-T cells, and short tandem repeat (STR) profiling authenticated them. To confirm that DAP10-engaged CAR-T cells could inhibit heterogeneous tumor cell growth, we generated GPC3-tdTomato-expressing SK-Hep1 cells. All cells were incubated at 37°C in a humidified atmosphere containing 5% carbon dioxide.

CAR vector construction and generation of CAR-T cells

Four CAR vectors were constructed into the pWPXLD backbone with EGFP by gene synthesis. The DAP10BBz was generated by fusing DAP10 (aa 1–93) with the 4-1BB (aa 214–255) and CD3ζ (aa 52–164) activation domains. The bispecific CAR was composed of a specific target-binding domain (anti-GPC3 scFv), DAP10 (aa 19–93), and classic CAR intracellular segments (4-1BB and CD3ζ). Conventional CAR vectors were constructed as previously described.[33] Lentiviruses were packaged in the HEK-293T cell line cotransfected with the pSPAX2, pMD2G, and CAR vectors in 10-cm dishes at a ratio of 4:1:3 (total amount: 24 μg). Lentivirus-containing supernatants were harvested at 48 h and 72 h post-transfection and filtered through 0.45-μm filters.

Human T cells were isolated from peripheral blood mononuclear cells (PBMCs) with human T cell-negative enrichment kits (STEMCELL Technologies, Vancouver, BC, Canada) and were activated with commercial expansion kits (Miltenyi Biotec, Bergisch Gladbach, Germany), followed by lentiviral transduction to generate CAR-T cells. CAR-T cells were maintained in GT-T551 H3 medium (Takara Bio, Shiga, Japan) containing 5% FBS, 100 U/mL penicillin (Gibco), 100 mg/mL streptomycin (Gibco), and 300 IU/ml hIL-2 (Quangang Pharmaceutical, Shandong, China). The healthy PBMC donors were provided inform consent for the use of their samples for research purposes, and all procedures were approved by the Research Ethics Board of the Guangzhou Institutes of Biomedicine and Health (GIBH).

NK cells isolation and culture

NK cells were stimulated with NK cell expansion kits (Miltenyi Biotec) following isolation from PBMCs with an NK cell

Figure 4. CAR GPC3-DAP10-T cells exhibit dual-antigen-targeting capacity *in vivo*

(A) Schematic diagram of the experiment. 1×10^6 HeLa cells were transplanted into NSI mice on. 5×10^6 CAR-T cells were transferred via tail-vein injection on day 0. Mice were mercifully killed on day 39. (B) Measurement of HeLa tumor volumes after treatment with 5×10^6 CAR19-T, DAP10-T, CAR GPC3-T, and CAR GPC3-DAP10-T cells (n = 6/group). (C) Spider plots of tumor volumes. (D) Tumor weights of the CAR19-T, DAP10-T, CAR GPC3-T, and CAR GPC3-DAP10-T cell groups on day 39 after CAR-T cell injection (time of sacrifice). (E) Schematic diagram of the experiment. 1×10^6 Huh7 cells were injected subcutaneously into NSI mice. (F) Measurement of Huh7 tumor volumes after treatment with 5×10^6 CAR19-T, DAP10-T, CAR GPC3-T, and CAR GPC3-DAP10-T cells through tail vein (n = 5/group). (G) The tumor-growth spider plots. (H) Mice were euthanized, and tumor tissues of the CAR19-T, DAP10-T, CAR GPC3-T, and CAR GPC3-DAP10-T cells were weighed on day 18 after CAR-T cell injection. Statistics: (B and F) the overall tumor-volume results were compared by two-way ANOVA with Tukey's multiple comparisons test. (D and H) Student's t test. Error bars denote the SEM. *$p < 0.05$, **$p < 0.01$, ***$p < 0.001$, ****$p < 0.0001$.

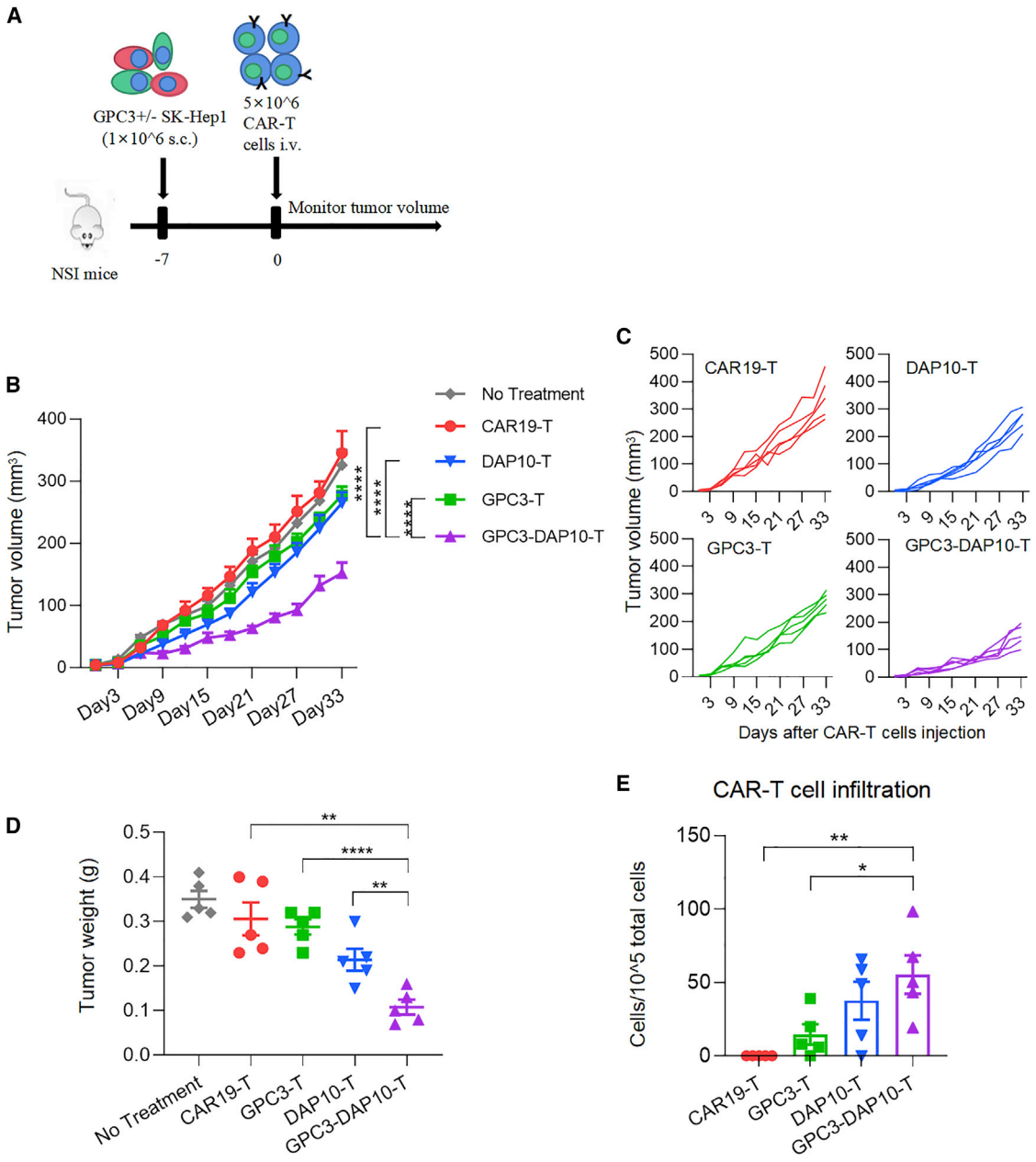

Figure 5. CAR GPC3-DAP10-T cells can eliminate heterogeneous cancer *in vivo*

(A) Schematic diagram of the experiment. 5×10^5 GPC3+tdTomato+ SK-Hep1 cells and 5×10^5 GPC3-EGFP+ SK-Hep1 cells were mixed and transplanted into NSI mice. 5×10^6 CAR-T cells were injected via tail vein on day 0 when the tumor nodules were palpable. Mice were mercifully killed on day 33. (B) Measurement of SK-Hep1 tumor volumes after treatment with CAR19-T, DAP10-T, CAR GPC3-T, and CAR GPC3-DAP10-T cells. (C) Individual tumor responses to CAR-T cell injection are shown. (D) Tumor weights of the CAR19-T, DAP10-T, CAR GPC3-T, and CAR GPC3-DAP10-T cell groups on day 33 (time of sacrifice). (E) CAR-T cell infiltration in the tumor tissue harvested from mice. Tumor volumes were compared by two-way ANOVA with Tukey's multiple comparisons test. Student's t test was employed for tumor weights and CAR-T cell infiltration comparison. Error bars denote the SEM. *$p < 0.05$, **$p < 0.01$, ***$p < 0.001$, ****$p < 0.0001$.

enrichment kit (STEMCELL Technologies). NK cells were cultured in GT-T551 H3 medium (Takara) containing 5% FBS, 100 U/mL penicillin, 100 mg/mL streptomycin, and hIL-2 (300 IU/ml).

NKG2D blocking assay

NKG2D blocking antibody (clone 1D11) and mouse IgG1κ isotype control antibody were purchased from BioLegend (San Diego, CA, USA). T cells and NK cells were incubated with the blocking antibody

(5 μg/mL) for 30 min at room temperature. The blocking and isotype control antibodies were maintained at 5 μg/mL in the killing assay medium.

Flow cytometry

Tumor cell lines were collected and stained with anti-MICA/B-APC (BioLegend), anti-ULBP1-APC, anti-ULBP2/5/6-APC, anti-ULBP3-PE, and anti-ULBP4-APC (R&D Systems, Minneapolis, MN, USA) antibodies in fluorescence-activated cell sorting (FACS) buffer at 4°C for 30 min. The cells were washed twice with FACS buffer, followed by cytometric analysis. Anti-CD3, anti-CD8, anti-CD4, and anti-NKG2D antibodies were employed to test the NKG2D expression levels of T cells; these antibodies were purchased from BioLegend. Anti-CD56 and anti-CD16 antibodies were used to determine the purity of isolated NK cells. Flow-cytometry experiments were performed with an Agilent flow cytometer, a CytoFLEX S flow cytometer (Beckman Coulter, Brea, CA, USA), or a C6 flow cytometer (BD Bioscience, East Rutherford, NJ, USA). FlowJo v.10 software was used for data analysis.

Cytotoxicity assay

Target cell lines were generated by transduction with a GFP-2A-luciferase lentivirus. The cytotoxicity of CAR-expressing T cells to target cells was evaluated at 2:1 to 1:2 (effector-to-target) ratios by performing a coculture killing assay in complete RPMI-1640 medium without IL-2. After coculture for 24 h, cytotoxicity was determined by luminance detection with the addition of a luciferase substrate.

Heterogeneous cancers killing assay

To determine the capacity of bispecific CAR-T cells to kill heterogeneous cancers, 1×10^5 heterogeneously mixed SK-Hep1 cells (GPC3+tdTomato+ and GPC3-EGFP+ cells were mixed at ratio 2:1) were cocultured with 1×10^5 CAR-T cells in 24-well plates for 24 h. The plates were imaged (8×8 photos for one well with 10× lens was made montages) by plate scanning system ImageXpress Micro Confocal (Molecular Devices, San Jose, CA, USA). Seven individual photos on diagonal lines were used to calculate cell counts for one montage photo by ImageJ.

Cytokine detection assay

The supernatant was precollected from the group in the killing assay with the highest E/T ratio and cryopreserved at -20°C. The killing assay was performed as previously described. We used multiple soluble analytes assay kits (BioLegend) and traditional ELISA kits (DAKEWE, Beijing, China) to evaluate granzyme B, IL-2, and IFN-γ. Three cytokines testing kits for IL-2 (A4), IFN-γ (B4), and granzyme B (B6) were customized from BioLegend. The cytokine assays were quantified using a flow cytometer. The results were analyzed with data analysis software suite online (https://www.biolegend.com/en-us/legendplex). The traditional ELISA was performed according to the manufacturer's protocols.

Animal experiments

NSI mice were bred and maintained in a specific pathogen-free animal center on a 12-h dark/12-h light cycle. All animal experiments were approved by the relevant Institutional Animal Care and Use Committee (IACUC).

For the cell-line-based xenograft models, 1×10^6 HeLa cells or Huh7 cells in 100 μL PBS were injected subcutaneously into the left flank of NSI mice (6–8 weeks old). When the tumor nodules were tangible, the mice were divided into 5 groups and injected with 100 μL PBS containing 5×10^6 CAR-T cells via tail-vein injection. Tumor length and width were measured every 3 days with calipers to calculate tumor volume (volume = (length × width^2)/2). The mice were killed before the tumor size reached the humane cutoff. Tumor tissues were weighed and processed for cytometric testing.

For the heterogeneous cell line xenograft models, 5×10^5 GPC3+ tdTomato+ SK-Hep1 cells and 5×10^5 GPC3-EGFP+ SK-Hep1 cells were mixed and transplanted into the right flank of NSI mice (6–8 weeks old). 5×10^6 CAR-T cells were injected into mouse via tail-vein injection when the tumor nodules were tangible. The observation experiments were performed as described above. In order to know the CAR-T cell infiltration, the tumor tissues were processed for cytometric testing.

Statistical analysis

Experiment data are shown as the mean ± SEM. Student's t test was used to determine the significance of differences between samples. Two-way ANOVA was used to determine the significance of differences among groups. A p value <0.05 was considered to indicate a significant difference. Analyses were carried out using GraphPad Prism software v.8.4.0 (GraphPad, San Diego, CA, USA).

Ethics statement

This study was carried out in accordance with the recommendations of the Laboratory Animal Center of the GIBH. The protocol was approved by the Animal Welfare Committee of GIBH.

SUPPLEMENTAL INFORMATION

Supplemental information can be found online at https://doi.org/10.1016/j.omto.2022.06.003.

ACKNOWLEDGMENTS

This study was supported by National Key Research and Development Plan nos. 2021YFE0202800 (P.L), 2017YFE0131600 (Y.L.), and 2019YFA0111500 (X.L.); National Natural Science Foundation of China nos. 82101928 (R.Z.), 81961128003 (P.L.), 81972672 (P.L.), 81773301 (Z.J.), 81870121(P.L.), 81873847 (J.Y.), and 32170946 (Z.J.); the Youth Innovation Promotion Association of the Chinese Academy of Sciences (2020351, Z.J.); Guangdong Basic and Applied Basic Research Foundation 2020A1515110403 (R.Z.); Guangdong Provincial Significant New Drugs Development no. 2019B020202003 (P.L.); Guangdong Basic and Applied Basic Research Foundation nos. 2019A1515010062 (Y.Y.), 2020A1515011516 (X.W.), 2021A1515110005(L.Q.), 2021A1515220077(S.Liu.), 2022A1515012569 (Z.J.), 2022A1515012484 (S.Liu.), 2022A1515012360 (L.Q.), 2022A1515010604 (Y.Y.), and 2020B1212060052; Guangzhou Science and

Technology Plan Project nos. 201907010042 (P.L.), 202102080470 (Y.Y.), and 2020B1212060052; Frontier Research Program of Guangzhou Regenerative Medicine and Health Guangdong Laboratory no. 2018GZR110105003 (P.L.); Science and Technology Program of Guangzhou, China (202002020083, X.L.); and the Open project of State Key Laboratory of Respiratory Disease, SKLRD-OP-202002 (Z.Z.). This work was partially supported by a grant from the University Grants Committee/Research Grants Council of the Hong Kong Special Administrative Region, China (project no. AoE/M-401/20). We acknowledge the Innovation and Technology Fund (ITF) and The Youth Talent Promotion project of Guangzhou Association for Science and Technology no. X20210201015 (Y.T.). The graphical abstract was created with BioRender.com. Finally, we would like to thank all the members in this list and their lab members for experimental materials, technical assistance, helpful discussions, and comments.

AUTHOR CONTRIBUTIONS

S.L., R.Z., and P.L. contributed to the conception and design; the collection and/or assembly of data; data analysis and interpretation; and manuscript writing. Q.W., Yao.L., S.W., and D.H. provided animal care and administrative support. D.Z., L.Q., Y.C., Y.L., Z.J., M.Z., J.S., M.L., X.W., Z.T., S.Liu., L.-H.Y., and Z.Z. contributed to the conception and design of the study. Y.Y., Y.L., P.L., and Q.T. contributed to the conception and design of the study; data analysis and interpretation; manuscript writing; and the final approval of the manuscript and provided financial support. All authors read and approved the final manuscript.

DECLARATION OF INTERESTS

The authors declare that they have no conflict of interests.

REFERENCES

1. Anagnostou, T., Riaz, I.B., Hashmi, S.K., Murad, M.H., and Kenderian, S.S. (2020). Anti-CD19 chimeric antigen receptor T-cell therapy in acute lymphocytic leukaemia: a systematic review and meta-analysis. Lancet Haematol. *7*, e816–e826. https://doi.org/10.1016/s2352-3026(20)30277-5.

2. Grupp, S.A., Kalos, M., Barrett, D., Aplenc, R., Porter, D.L., Rheingold, S.R., Teachey, D.T., Chew, A., Hauck, B., Wright, J.F., et al. (2013). Chimeric antigen receptor-modified T cells for acute lymphoid leukemia. N. Engl. J. Med. *368*, 1509–1518. https://doi.org/10.1056/nejmoa1215134.

3. Mohty, M., Gautier, J., Malard, F., Aljurf, M., Bazarbachi, A., Chabannon, C., Kharfan-Dabaja, M.A., Savani, B.N., Huang, H., Kenderian, S., et al. (2019). CD19 chimeric antigen receptor-T cells in B-cell leukemia and lymphoma: current status and perspectives. Leukemia *33*, 2767–2778. https://doi.org/10.1038/s41375-019-0615-5.

4. Ghahri-Saremi, N., Akbari, B., Soltantoyeh, T., Hadjati, J., Ghassemi, S., and Mirzaei, H.R. (2021). Genetic modification of cytokine signaling to enhance efficacy of CAR T cell therapy in solid tumors. Front. Immunol. *12*, 738456. https://doi.org/10.3389/fimmu.2021.738456.

5. Johnson, A.J., Wei, J., Rosser, J.M., Künkele, A., Chang, C.A., Reid, A.N., and Jensen, M.C. (2021). Rationally designed transgene-encoded cell-surface polypeptide tag for multiplexed programming of CAR T-cell synthetic outputs. Cancer Immunol. Res. *9*, 1047–1060. https://doi.org/10.1158/2326-6066.cir-20-0470.

6. Rousso-Noori, L., Mastandrea, I., Talmor, S., Waks, T., Globerson Levin, A., Haugas, M., Teesalu, T., Alvarez-Vallina, L., Eshhar, Z., and Friedmann-Morvinski, D. (2021). P32-specific CAR T cells with dual antitumor and antiangiogenic therapeutic potential in gliomas. Nat. Commun. *12*, 3615. https://doi.org/10.1038/s41467-021-23817-2.

7. Rezvani, K., Rouce, R., Liu, E., and Shpall, E. (2017). Engineering natural killer cells for cancer immunotherapy. Mol. Ther. *25*, 1769–1781. https://doi.org/10.1016/j.ymthe.2017.06.012.

8. Lanier, L.L. (1998). NK cell receptors. Annu. Rev. Immunol. *16*, 359–393. https://doi.org/10.1146/annurev.immunol.16.1.359.

9. Raulet, D.H., and Held, W. (1995). Natural killer cell receptors: the offs and ons of NK cell recognition. Cell *82*, 697–700. https://doi.org/10.1016/0092-8674(95)90466-2.

10. Biassoni, R. (2008). Natural killer cell receptors. Adv. Exp. Med. Biol. *640*, 35–52. https://doi.org/10.1007/978-0-387-09789-3_4.

11. Dhar, P., and Wu, J.D. (2018). NKG2D and its ligands in cancer. Curr. Opin. Immunol. *51*, 55–61. https://doi.org/10.1016/j.coi.2018.02.004.

12. Liu, H., Wang, S., Xin, J., Wang, J., Yao, C., and Zhang, Z. (2019). Role of NKG2D and its ligands in cancer immunotherapy. Am. J. Cancer Res. *9*, 2064–2078.

13. González, S., López-Soto, A., Suarez-Alvarez, B., López-Vázquez, A., and López-Larrea, C. (2008). NKG2D ligands: key targets of the immune response. Trends Immunol. *29*, 397–403. https://doi.org/10.1016/j.it.2008.04.007.

14. Lanier, L.L. (2015). NKG2D receptor and its ligands in host defense. Cancer Immunol. Res. *3*, 575–582. https://doi.org/10.1158/2326-6066.cir-15-0098.

15. Markiewicz, M.A., Carayannopoulos, L.N., Naidenko, O.V., Matsui, K., Burack, W.R., Wise, E.L., Fremont, D.H., Allen, P.M., Yokoyama, W.M., Colonna, M., and Shaw, A.S. (2005). Costimulation through NKG2D enhances murine CD8+ CTL function: similarities and differences between NKG2D and CD28 costimulation. J. Immunol. *175*, 2825–2833. https://doi.org/10.4049/jimmunol.175.5.2825.

16. Groh, V., Rhinehart, R., Randolph-Habecker, J., Topp, M.S., Riddell, S.R., and Spies, T. (2001). Costimulation of CD8αβ T cells by NKG2D via engagement by MIC induced on virus-infected cells. Nat. Immunol. *2*, 255–260. https://doi.org/10.1038/85321.

17. Dargel, C., Bassani-Sternberg, M., Hasreiter, J., Zani, F., Bockmann, J.H., Thiele, F., Bohne, F., Wisskirchen, K., Wilde, S., Sprinzl, M.F., et al. (2015). T cells engineered to express a T-cell receptor specific for glypican-3 to recognize and kill hepatoma cells in vitro and in mice. Gastroenterology *149*, 1042–1052. https://doi.org/10.1053/j.gastro.2015.05.055.

18. Ye, W., Jiang, Z., Li, G.X., Xiao, Y., Lin, S., Lai, Y., Wang, S., Li, B., Jia, B., Li, Y., et al. (2015). Quantitative evaluation of the immunodeficiency of a mouse strain by tumor engraftments. J. Hematol. Oncol. *8*, 59. https://doi.org/10.1186/s13045-015-0156-y.

19. Miao, L., Zhang, Z., Ren, Z., Tang, F., and Li, Y. (2021). Obstacles and coping strategies of CAR-T cell immunotherapy in solid tumors. Front. Immunol. *12*, 687822. https://doi.org/10.3389/fimmu.2021.687822.

20. Kirtane, K., Elmariah, H., Chung, C.H., and Abate-Daga, D. (2021). Adoptive cellular therapy in solid tumor malignancies: review of the literature and challenges ahead. J. Immunother. Cancer *9*, e002723. https://doi.org/10.1136/jitc-2021-002723.

21. Yu, M.W., and Quail, D.F. (2021). Immunotherapy for glioblastoma: current progress and challenges. Front. Immunol. *12*, 676301. https://doi.org/10.3389/fimmu.2021.676301.

22. Zhao, J., Song, Y., and Liu, D. (2019). Clinical trials of dual-target CAR T cells, donor-derived CAR T cells, and universal CAR T cells for acute lymphoid leukemia. J. Hematol. Oncol. *12*, 17. https://doi.org/10.1186/s13045-019-0705-x.

23. Yang, D., Sun, B., Dai, H., Li, W., Shi, L., Zhang, P., Li, S., and Zhao, X. (2019). T cells expressing NKG2D chimeric antigen receptors efficiently eliminate glioblastoma and cancer stem cells. J. Immunother. Cancer *7*, 171. https://doi.org/10.1186/s40425-019-0642-9.

24. Sentman, C.L., and Meehan, K.R. (2014). NKG2D CARs as cell therapy for cancer. Cancer J. *20*, 156–159. https://doi.org/10.1097/ppo.0000000000000029.

25. Sun, B., Yang, D., Dai, H., Liu, X., Jia, R., Cui, X., Li, W., Cai, C., Xu, J., and Zhao, X. (2019). Eradication of hepatocellular carcinoma by NKG2D-based CAR-T cells. Cancer Immunol. Res. *7*, 1813–1823. https://doi.org/10.1158/2326-6066.cir-19-0026.

26. Curio, S., Jonsson, G., and Marinović, S. (2021). A summary of current NKG2D-based CAR clinical trials. Immunother. Adv. *1*, ltab018. https://doi.org/10.1093/immadv/ltab018.

27. Baumeister, S.H., Murad, J., Werner, L., Daley, H., Trebeden-Negre, H., Gicobi, J.K., Schmucker, A., Reder, J., Sentman, C.L., Gilham, D.E., et al. (2019). Phase I trial of autologous CAR T cells targeting NKG2D ligands in patients with AML/MDS and

multiple myeloma. Cancer Immunol. Res. *7*, 100–112. https://doi.org/10.1158/2326-6066.cir-18-0307.

28. Yang, F., Shao, Y., Yang, F., Liu, M., Huang, J., Zhu, K., Guo, C., Luo, J., Li, W., Yang, B., et al. (2013). Valproic acid upregulates NKG2D ligand expression and enhances susceptibility of human renal carcinoma cells to NK cell-mediated cytotoxicity. Arch. Med. Sci. *2*, 323–331. https://doi.org/10.5114/aoms.2013.34413.

29. Paczulla, A.M., Rothfelder, K., Raffel, S., Konantz, M., Steinbacher, J., Wang, H., Tandler, C., Mbarga, M., Schaefer, T., Falcone, M., et al. (2019). Absence of NKG2D ligands defines leukaemia stem cells and mediates their immune evasion. Nature *572*, 254–259. https://doi.org/10.1038/s41586-019-1410-1.

30. Schmudde, M., Braun, A., Pende, D., Sonnemann, J., Klier, U., Beck, J.F., Moretta, L., and Bröker, B.M. (2008). Histone deacetylase inhibitors sensitize tumour cells for cytotoxic effects of natural killer cells. Cancer Lett. *272*, 110–121. https://doi.org/10.1016/j.canlet.2008.06.027.

31. Valés-Gómez, M., Chisholm, S.E., Cassady-Cain, R.L., Roda-Navarro, P., and Reyburn, H.T. (2008). Selective induction of expression of a ligand for the NKG2D receptor by proteasome inhibitors. Cancer Res. *68*, 1546–1554. https://doi.org/10.1158/0008-5472.can-07-2973.

32. Abruzzese, M.P., Bilotta, M.T., Fionda, C., Zingoni, A., Soriani, A., Vulpis, E., Borrelli, C., Zitti, B., Petrucci, M.T., Ricciardi, M.R., et al. (2016). Inhibition of bromodomain and extra-terminal (BET) proteins increases NKG2D ligand MICA expression and sensitivity to NK cell-mediated cytotoxicity in multiple myeloma cells: role of cMYC-IRF4-miR-125b interplay. J. Hematol. Oncol. *9*, 134. https://doi.org/10.1186/s13045-016-0362-2.

33. Lai, Y., Weng, J., Wei, X., Qin, L., Lai, P., Zhao, R., Jiang, Z., Li, B., Lin, S., Wang, S., et al. (2018). Toll-like receptor 2 costimulation potentiates the antitumor efficacy of CAR T Cells. Leukemia *32*, 801–808. https://doi.org/10.1038/leu.2017.249.